New Results on Structure Effects in Nuclear Fission

K.-H. Schmidt[a], J. Benlliure[b], C. Böckstiegel[c], H.-G. Clerc[c], A. Grewe[c], A. Heinz[c*], A. V. Ignatyuk[d], A. R. Junghans[a†], M. de Jong[c], J. Müller[c], M. Pfützner[e], F. Rejmund[f], S. Steinhäuser[c], B. Voss[a]

[a]Gesellschaft für Schwerionenforschung, Planckstraße 1, 64291 Darmstadt, Germany
[b]Faculdad de Fisica, Universidad de Santiago de Compostela, 15706 Santiago de Compostela, Spain
[c]Institut für Kernphysik, Technische Universität Darmstadt, Schloßgartenstraße 9, 64289 Darmstadt
[d]Institute of Physics and Power Engineering, 249020 Obninsk, Kaluga region, Russia
[e]Instytut Fizyki Doswiadczalney, Uniwersytet Warszawaski, ul Hoza 69, 00-381 Warszawa, Poland
[f]Institut de Physique Nucléaire, IN2P3, 92406 Orsay-Cedex, France

The secondary-beam facility of GSI provided the technical equipment for a new kind of fission experiment. Fission properties of short-lived neutron-deficient nuclei have been investigated in inverse kinematics. The measured element distributions reveal new kinds of systematics on shell structure and even-odd effects and lead to an improved understanding of strucure effects in nuclear fission.

1. INTRODUCTION

Nuclear fission is one of the most intensively studied types of nuclear reaction [1,2], but still the experimental knowledge is rather incomplete. In the last three years, important progress was achieved on this field by use of the new experimental facilities of GSI. In the present contribution, an overview on these new results is given.

Low-energy fission is a nuclear reaction at the extremes. But unlike many other studies, which try to reach the highest temperatures in nuclear systems, fission may start at zero temperature. It is a dramatic reordering of cold nuclear matter. It may start in the ground state as spontaneous fission and proceed by tunnelling through the fission barrier. Even when starting from excitation energies close to the fission barrier, the system has to pass through cold transition states at the barrier.

Fission offers unique conditions to study:
The interplay of nuclear structure and dynamics.
Phenomena of nuclear structure at extreme deformation.
The onset of dissipation in cold nuclei.

* Present address: Argonne National Laboratory, Physics Division, Building 203, 9700 South Cass Avenue, ARGONNE, IL 60439, U.S.A.
† Present address: Nuclear Physics Laboratory, BOX 354290, University of Washington, SEATTLE, WA 98195, U.S.A.

The fission process yields many observables, but here we restrict to the fission-fragment distributions in Z and A. The understanding of the isotopic production in fission has acquired a renewed interest since its application for the production of neutron-rich secondary beams in next-generation secondary-beam facilities is intensively discussed.

In the following, we will shortly summarise the actual experimental situation and the present understanding of main structure effects in fission.

2. PREVIOUS KNOWLEDGE

An important systematics on mass distributions of fission fragments has been presented in 1974 by Unik and collaborators [3]. All nuclei from ^{229}Th to ^{254}Es were found to fission into fragments with strongly different mass. Symmetric fission is strongly suppressed. The mean mass of the heavy component is almost stationary. Obviously, this asymmetric fission is controlled by shell effects in the heavy fragment. The most important shells are considered to be the spherical N=82 shell and a shell at N≈90 at large deformation (β≈0.6) [4].

We find this region of asymmetric fission again on the chart of the nuclides (Fig. 1), which summarises the actual status of experimental knowledge on fission-fragment distributions. Only those systems measured at excitation energies less than 10 MeV above the fission barrier are included. From ^{227}Ra up to ^{256}Fm, the mass distributions are double-humped. But the asymmetric fission dies out on both extremes of the mass range. There is a dramatic change of the mass distribution to a narrow single-humped distribution found in ^{258}Fm [5]. This is explained by the formation of two spherical nuclei close to the doubly magic ^{132}Sn. Selected nuclei in this range are accessible to experiment because they decay by spontaneous fission.

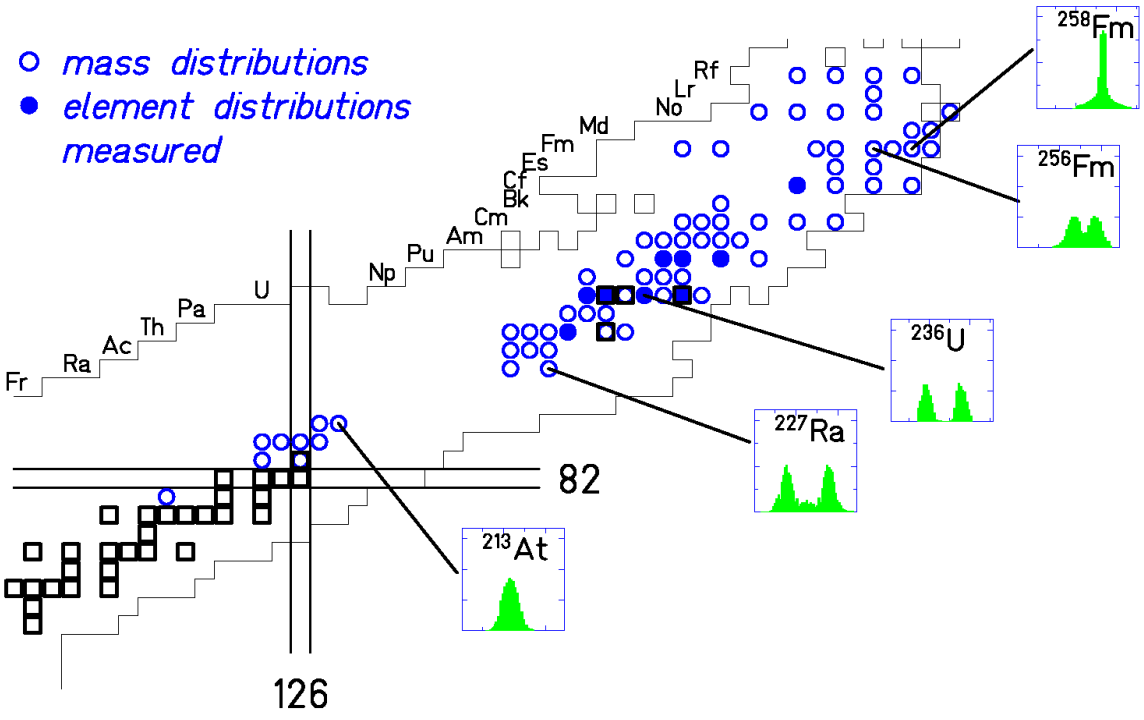

Fig. 1: Survey on the mass and element distributions measured in previous fission experiments for excitation energies less than 10 MeV above the fission barrier.

But also at the lower end one observes single-humped distributions, e.g. for ^{213}Ac. However, these are much broader. A few mass distributions from low excitation energies could be measured by use of radioactive targets ^{226}Ra and ^{227}Ac (see e.g. [6]). Some nuclei in the suspected transition region between ^{225}Ac and ^{213}At have been produced with excitation energies around 30 MeV by fusion reactions [7,8,9].

It is obvious that our experimental knowledge on nuclear fission is rather incomplete. Mass distributions have been measured for only 78 nuclei. Element distributions are a more direct signature of fission, because they are not modified by neutron evaporation from the excited fission fragments. They are measured with good resolution by in-flight methods for 9 fissioning nuclei only.

Most of the research activity on nuclear fission has concentrated on a few nuclei, e.g. on ^{235}U and ^{239}Pu, to produce a tremendous amount of high-precision data necessary for the technical applications in nuclear reactors or in nuclear weapons. It becomes clear from Fig. 1 that, from a scientific point of view, the knowledge on nuclear fission is still rather scarce.

3. SECONDARY-BEAM EXPERIMENTS

In a conventional fission experiment, a target nucleus is excited, e.g. by neutrons, protons or photons. The fission fragments reach the detectors with a kinetic energy given by the fission process. Experiments on low-energy fission are limited by the available target materials. Up to now, spontaneous fission offers the only possibility to overcome this limitation for those nuclei of interest which can be produced e.g. by heavy-ion fusion reactions.

The secondary-beam facility of GSI allows now to become independent of available target nuclei. By fragmentation of a ^{238}U beam at 1 A GeV, many short-lived radioactive nuclei are produced. After isotopic separation in the fragment separator, several hundred fissile nuclei are available for nuclear-fission studies [10]. However, they leave the separator with energies of about 500 A MeV. Therefore, the experiment has to be performed in inverse kinematics. In our experiment, we excited the secondary projectiles by Coulomb excitation in the electromagnetic field of a heavy target nucleus. This leads to the excitation of the giant dipole resonance with a mean energy of 11 MeV and a non-negligible width. The width of the excitation-energy distribution is a certain disadvantage of the new method. It is the price to pay for the rather free choice of the secondary projectile. On the other hand, the inverse kinematics brings another advantage. The fission fragments reach the detectors with energies around 500 A MeV. At these energies, they are completely stripped, and their atomic number can be determined easily by a ΔE measurement with excellent resolution, see Fig. 2. As already mentioned above, the nuclear charge of the fragments, in contrast to the mass number, is a direct signature of the fission process. Fission induced by nuclear interactions is strongly suppressed by the condition that all protons of the secondary projectile are found in the fission fragments. A remaining contribution is subtracted using data from a low-Z target. A detailed description of the experimental technique is given in ref. [11].

4. EXPERIMENTAL RESULTS

The peaks of the ΔE spectrum (Fig. 2) corresponding to the different elements can be integrated to determine the element yields. This has been done for 70 fissioning nuclei. That means that, with the result of the secondary-beam experiment, the number of systems investigated in low-energy fission has almost doubled.

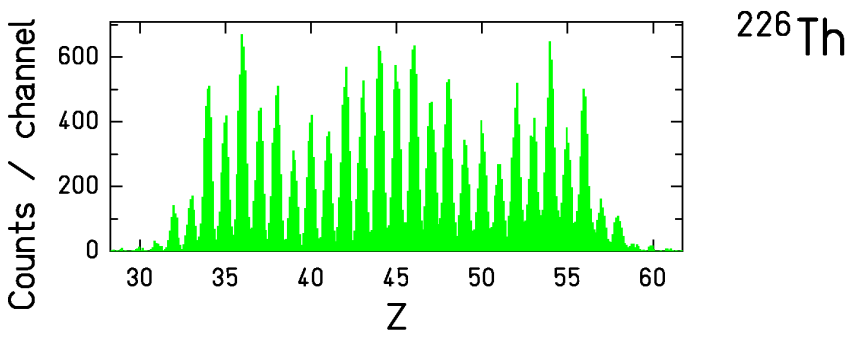

Fig. 2: Element distribution of the fission products of ^{226}Th, deduced from the signals of the ionisation chamber.

The systematic overview in Fig. 3 shows 28 systems in the transitional region from double-humped to single-humped distributions. The gradual transition is systematically mapped. Almost all these element distributions have been measured for the first time. In the centre, the two fission components compete with each other, leading to triple-humped distributions. In the following, the theoretical understanding of these results will be discussed.

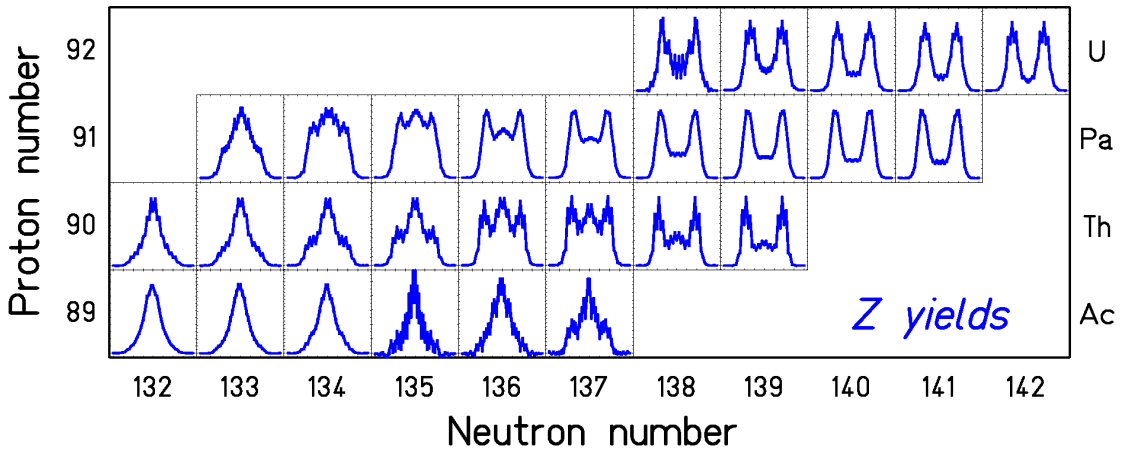

Fig. 3: Measured element distributions of fission fragments from electromagnetic-induced fission of 28 systems from ^{221}Ac to ^{234}U.

5. SIGNATURES OF SHELL EFFECTS IN NUCLEAR FISSION

The theoretical work on structure effects in fission presently concentrates on the most realistic description of the shape-dependent potential-energy surface (e.g. refs. [12,13]). The results look complicated, and the minimisation with respect to higher-order shape distortions even introduces hidden discontinuities. These discontinuities make it even more difficult to

perform full dynamical calculations in order to obtain quantitative predictions of the isotopic distributions of fission fragments. Up to now, these calculations only serve as a guide to qualitatively relate the structures in the data to the structures in the potential-energy landscape.

Since theory cannot yet provide us with a quantitative prediction, we tried to understand the data with a semi-empirical approach. The basic idea of our approach has been inspired by considerations of Itkis et al. [14]. We consider the fission barrier under the condition of a certain mass asymmetry. The height of the fission barrier $V(A)$ is calculated as the sum of a liquid-drop barrier and two shells. The liquid-drop barrier is minimum at symmetry and grows quadratically as a function of mass asymmetry. The shell effects appear at N=82 and N≈90. A more detailed description of the model is given in ref. [15]. This picture provides us with an explanation for the predominance of asymmetric fission of the actinides. ^{234}U serves as an example to show that the lowest fission barrier appears for asymmetric mass split. Approaching ^{264}Fm, the shell effects at N=82 in both fragments join, giving rise to a narrow symmetric mass distribution. In lighter nuclei, the influence of the shells on the fission process is weakened, because they add up to the higher liquid-drop potential at larger mass asymmetry. In ^{208}Pb, the fission barrier is lowest for symmetric mass splits.

A more quantitative description of this schematic model is given in Fig. 4. The mass yield $Y(A)$ is assumed to be proportional to the phase space $\rho(A)$ available above the fission barrier at a certain mass split. The initial excitation energy E^* above the mass-dependent barrier $V(A)$ is available for intrinsic excitations. The shell effect in the level density is washed out with energy as proposed by Ignatyuk et al. [16]. The stiffness C of the underlying liquid-drop potential is deduced from a systematics of the width of measured mass distributions [17]. The shells are modelled in a way that the calculated yields $Y(Z)$ for ^{227}Th are reproduced.

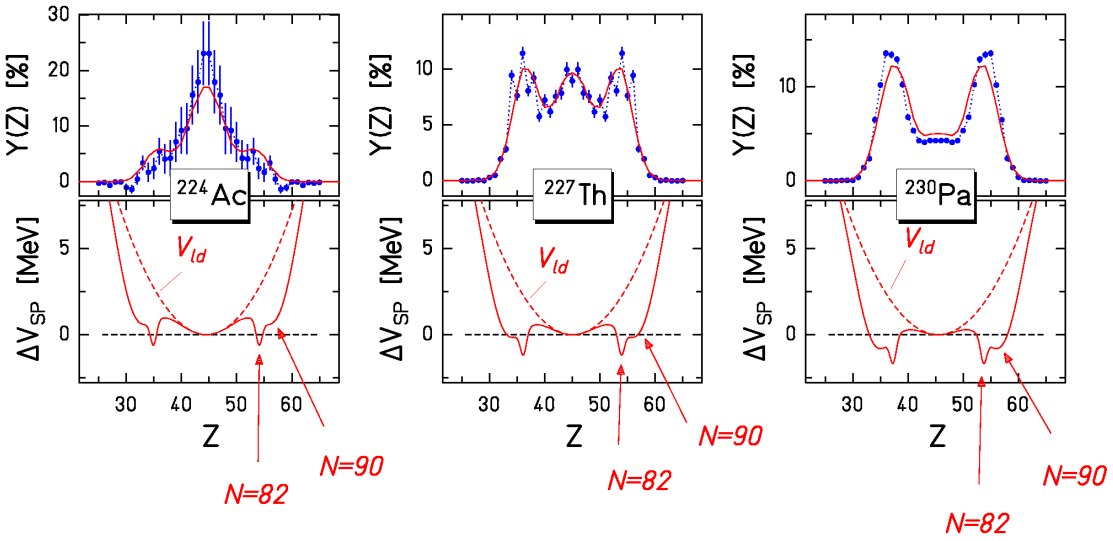

Fig. 4: Measured element yields compared to the model predictions (upper parts), and the assumed variation ΔV of the fission barrier as a function of the nuclear charge of one fission fragment with respect to the fission barrier for symmetric splits (lower parts).

Now the model is applied to other nuclei (^{224}Ac and ^{230}Pa) without any further adjustment. The shells move up and down on the liquid-drop potential just a little bit due to the shift in neutron number of the fissioning nucleus. These tiny variations are sufficient to substantially modify the shape of the element distribution just as much as the experimental distributions change. This good reproduction of the data is a strong argument that this model gives the correct explanation for basic features of the transition from asymmetric to symmetric fission.

Fig. 5 presents the element distributions, calculated with the same model, for all measured fissioning systems in comparison with the experimental data. There is an astonishingly good agreement for the whole systematics.

This success of the very simple model might indicate that the dynamics of the fission process tends to wash out the influence of the details of the potential-energy landscape. It is to be expected that due to the inertia of the collective motion the process does not feel every wiggle in the potential energy but rather takes a smooth trajectory.

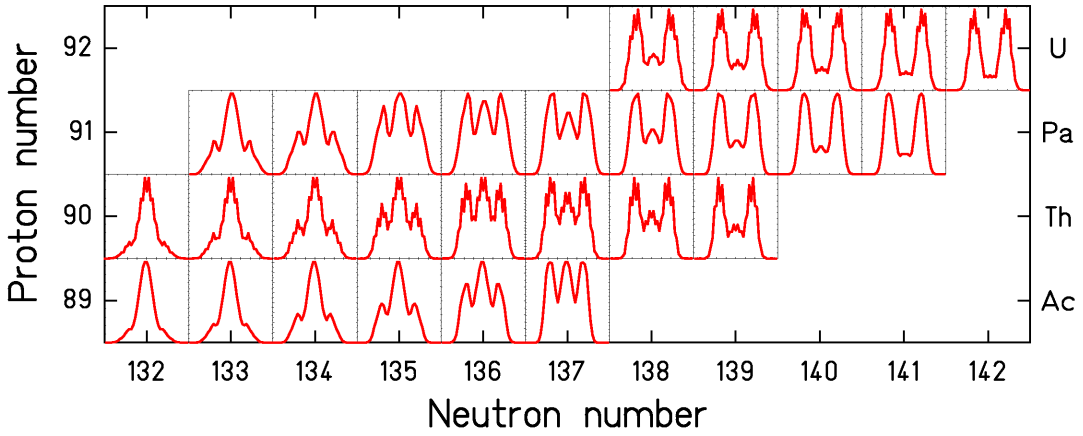

Fig. 5: Calculated element distributions of fission fragments from electromagnetic-induced fission of 28 systems from ^{221}Ac to ^{234}U.

6. SIGNATURES OF PAIRING CORRELATIONS IN NUCLEAR FISSION

Let us now address the even-odd structure found in the element distributions. Fig. 6 summarises the systematics of the global even-odd effect known prior to our experiment [2]. From the few measured systems one can deduce a gradual decrease of the even-odd effect with increasing Coulomb parameter $Z^2/A^{1/3}$. This tells us that the dissipation leads to higher probability of pair breaking for the heavier systems.

From the large number of element distributions measured in our experiment, we could deduce a few additional systematic trends. The first one is illustrated in Fig. 7. The left upper part shows the element distribution of ^{220}Ac. It looks smooth at the first sight. But an amplified view on the wings of the distribution reveals a strong even-odd structure. With respect to a smooth distribution, there is an enhanced production of even-Z elements in the light tail and an enhanced production of odd-Z elements in the heavy tail. The local even-odd structure can

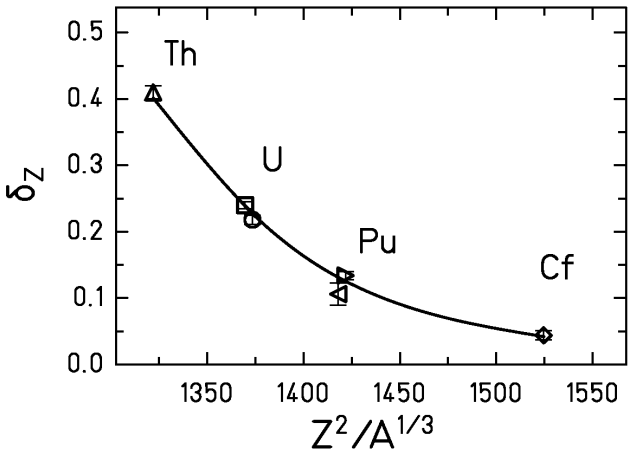

Fig. 6: Systematics of global even-odd effects in fission-fragment element yields.

quantitatively be determined by the logarithmic third difference δ_Z, introduced by Tracy et al. [18]. The local even-odd effect amounts to more than 20% in the wings. The same effect is found for ^{228}Pa. Also all the other odd-Z fissioning systems investigated show the same feature.

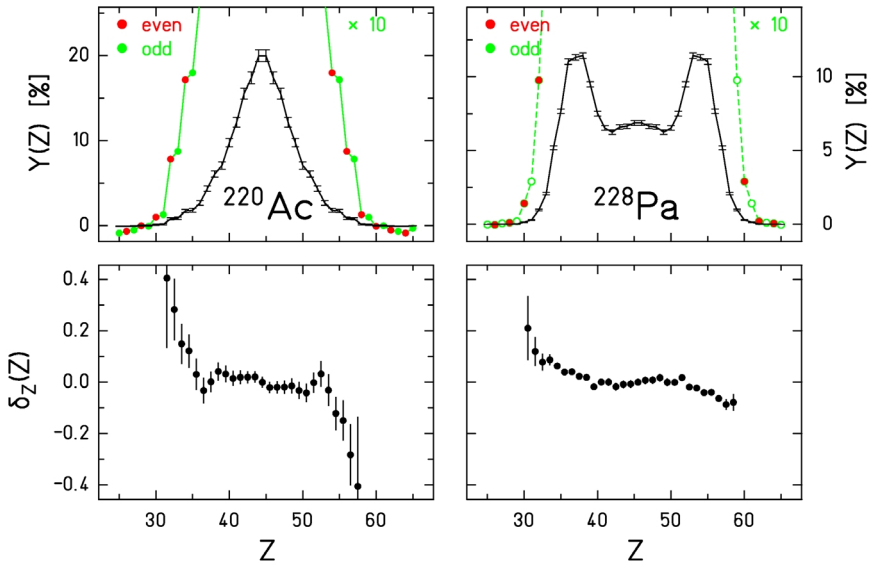

Fig. 7: Measured element distributions (upper part) and deduced local even-odd effect (lower part) after electromagnetic fission of ^{220}Ac and ^{228}Pa.

We conclude that the unpaired proton prefers to go to the heavy fragment. The explanation can probably be found in the larger value of the single-particle level density in the heavy fragment, which scales with the volume.

The secondary-beam experiment is the first one to yield the even-odd effect for symmetric charge splits. This allows to follow the variation of the even-odd effect in even-Z fissioning systems over a large range of charge asymmetry. We observe a strong increase of the local even-odd effect in the wings of the distribution as can be seen in Fig. 8 for ^{226}Th and ^{223}U. Also all the other even-Z fissioning systems show the same feature. We explain this finding again by the large single-particle level density in the heavier fragment. When one proton pair is broken, the unpaired protons both prefer the heavy fragment. Previously an increased local even-odd effect in extremely asymmetric fission found in ^{235}U(n_{th},f) was interpreted as a direct measure of the temperature at scission [19]. This interpretation must be revised on the basis of our new results [20].

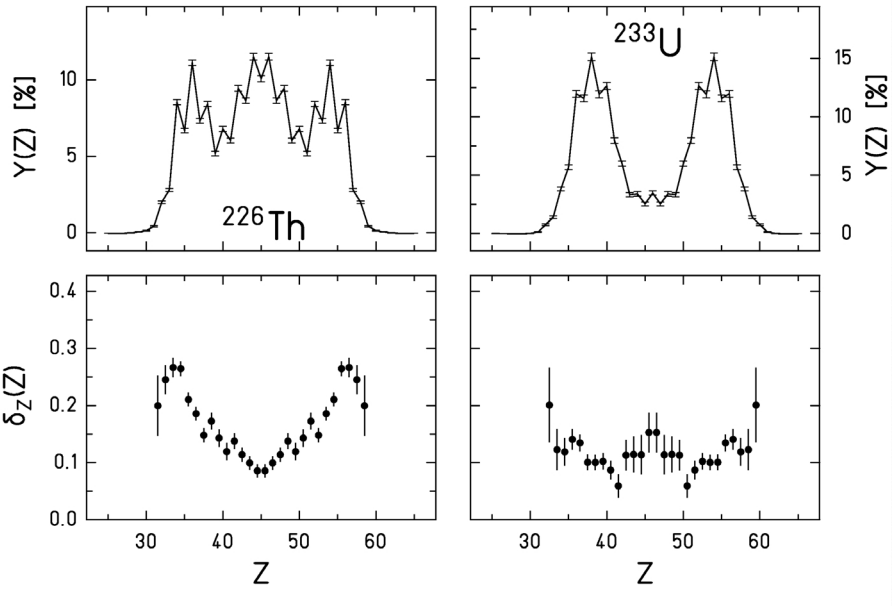

Fig. 8: Measured element distributions (upper part) and deduced local even-odd effect (lower part) after electromagnetic fission of ^{226}Th and ^{233}U.

The new features found in even-odd structures of fission-fragment distributions [20], which are not explained by any of the available models [21,22], motivated us to reconsider the theoretical understanding of pair breaking in fission [23]. These considerations allowed us to address a last topic, which refers to a new interpretation of a long-standing puzzle. Fission-fragment distributions measured at very high total kinetic energies allow to determine primary yields in proton and neutron number, since neutron evaporation is impossible or strongly suppressed. Data of this nature only exist for three systems, ^{233}U(n_{th},f), ^{235}U(n_{th},f) and ^{239}Pu(n_{th},f). The even-odd effect in proton number is found to be much larger than the even-odd effect in

neutron number. At the first sight, this is a surprising result, because the even-odd structures in proton and neutron number in the binding energies are about equal.

It is important to take into account that a cold nucleus is a two-component superfluid system. This is a very interesting and very specific property of nuclei. Therefore, the dissipation process in fission may lead to quasiparticle excitations and still one of the subsystems remains completely paired. In our new approach, we formulated the probability P_0^Z to preserve a completely paired proton configuration as the probability to store all the dissipated energy in the neutron subsystem. It is given by the partial level density of pure neutron excitations divided by the total level density. The probability P_0^N to preserve a completely paired neutron configuration can be calculated in an analogous way by the partial level density of pure proton excitations divided by the total level density. A rigorous formulation on the basis of the superfluid nuclear model results in the curves shown in Fig. 9. Due to the neutron excess in the fissioning nuclei, P_0^Z is much larger than P_0^N. When the measured even-odd effects in proton number are taken to determine the excitation energy at scission, the resulting even-odd effects in neutron number coincide rather well with the theoretical curve.

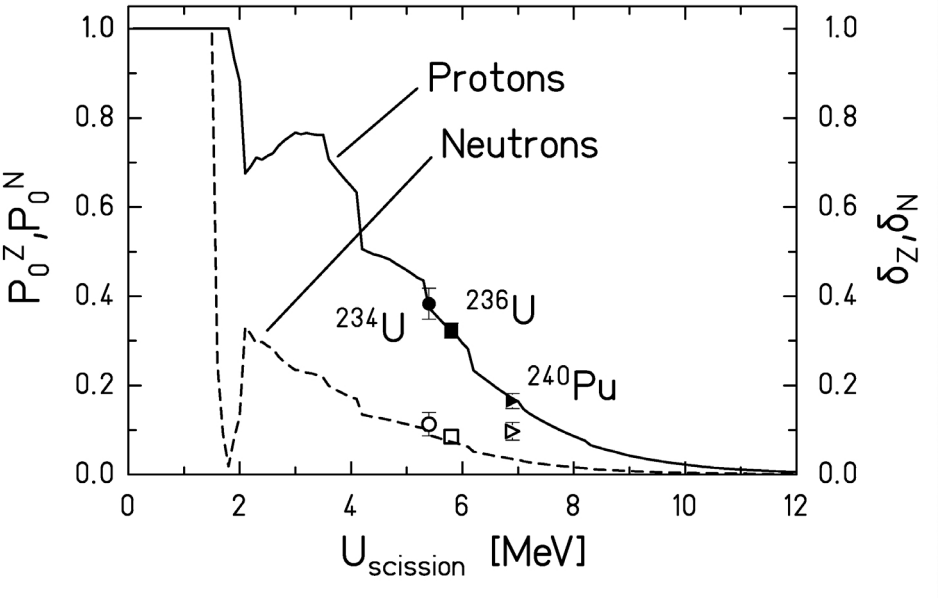

Fig. 9: Calculated survival probabilities of the completely paired proton and neutron configurations as a function of excitation energy at scission (left scale) and experimental data on the proton and neutron global even-odd effects at high kinetic energies of the light fragments (right scale) for the fissioning nuclei ^{234}U (Ekin = 111 MeV) [24], ^{236}U (Ekin=108 MeV) [25], and ^{240}Pu (Ekin = 111 MeV) [26].

7. SUMMARY

We would like to stress that nuclear fission is a unique laboratory. There are two essential very specific features which are not found in other systems, e.g. in the decay of metallic clusters. Firstly, the electric charge in nuclei is homogeneously distributed over the whole vol-

ume. This gives rise to a “true” fission process which is essentially symmetric. Shell effects modulate this feature. Secondly, cold nuclei are two-component superfluid systems. This gives rise to particularly complex features in pair breaking.

Experiments with secondary beams using elaborate experimental installations available at GSI opened up new possibilities for experimental studies of nuclear fission. New systematic results for a continuous region of fissioning systems have been obtained.

The new results are consistent with statistical concepts to an astonishingly high degree.

Although the full understanding of the dynamics of fission is still missing, one came closer to a quantitative description of structure effects in fission.

REFERENCES

1. R. Vandenbosch, J. R. Huizenga, Nuclear Fission (New York: Academic), 1973.
2. The Nuclear Fission Process, C. Wagemans, ed., CRC Press, London, 1991.
3. J. P. Unik, J. E. Gindler, L. E. Glendenin, K. F. Flynn, A. Gorski, R. K. Sjoblom, Proc. Symp. on Physics and Chem. of Fission, Rochester 1973, IAEA Vienna (1974), Vol. 2, p. 19.
4. B. D. Wilkins, E. P. Steinberg, R. R. Chasman, Phys. Rev. C 14 (1976) 1832.
5. D. C. Hoffman, M. R. Lane, Radiochimica Acta 70/71 (1995) 135.
6. H. J. Specht, Phys. Scripta 10A (1974) 21.
7. I. Nishinaka, Y. Nagame, K. Tsukada, H. Ikezoe, K. Sueki, H. Nakahara, M. Tanikawa, T. Ohtsuki, Phys. Rev. C 56 (1997) 891.
8. I. V. Pokrovsky, L. Calabretta, M. G. Itkis, N. A. Kondratiev, E. M. Kozulin, C. Maiolino, E. V. Prokhorova, A. Ya. Rusanov, S. P. Tretyakova, Phys. Rev. C 60 (1999) 041304.
9. I. V. Pokrovsky, M. G. Itkis, J. M. Itkis, N. A. Kondratiev, E. M. Kozulin, E. V. Prokhorova, V. S. Salamatin, V. V. Pashkevich, S. I. Mulgin, A. Ya. Rusanov, S. V. Zhdanov, G. G. Chubarian, B. J. Hurst, R. P. Schmitt, C. Agodi, G. Bellia, L. Calabretta, K. Lukashin, C. Maiolino, A. Kelic, G. Rudolf, L. Stuttge, F. Hanappe, Phys. Rev. C 62 (2000) 014615.
10. K.-H. Schmidt, A. Heinz, H.-G. Clerc, B. Blank, T. Brohm, S. Czajkowski, C. Donzaud, H. Geissel, E. Hanelt, H. Irnich, M. C. Itkis, M. de Jong, A. Junghans, A. Magel, G. Münzenberg, F. Nickel, M. Pfützner, A. Piechaczek, C. Roehl, C. Scheidenberger, W. Schwab, S. Steinhäuser, K. Sümmerer, W. Trinder, B. Voss, S. V. Zhdanov, Phys. Lett. B 325 (1994) 313.
11. K.-H. Schmidt, S. Steinhäuser, C. Böckstiegel, A. Grewe, A. Heinz, A. R. Junghans, J. Benlliure, H.-G. Clerc, M. de Jong, J. Müller, M. Pfützner, B. Voss, Nucl. Phys. A 665 (2000) 221.
12. V. V. Pashkevich, Nucl. Phys. A 477 (1988) 1.
13. P. Möller, A. Iwamoto, Phys. Rev. C 61 (2000) 047602.
14. M. G. Itkis, V. N. Okolovich, A. Ya. Rusanov, G. N. Smirenkin, Sov. J. Part. Nucl. 19 (1988) 301.
15. J. Benlliure, A. Grewe, M. de Jong, K.-H. Schmidt, S. Zhdanov, Nucl. Phys. A 628 (1998) 458.
16. A. V. Ignatyuk, G. N. Smirenkin, A. S. Tiskin, Yad. Fiz. 21 (1975) 485 (Sov. J. Nucl. Phys. 21 (1975) 255).
17. S. I. Mulgin, K.-H. Schmidt, A. Grewe, S. V. Zhdanov, Nucl. Phys. A 640 (1998) 375.

18. B. L. Tracy, J. Chaumont, R. Klapisch, J. M. Nitschke, A. M. Poskanzer, E. Roeckl, C. Thibault, Phys. Rev. C 5 (1972) 222.
19. J. L. Sida, P. Armbruster, M. Bernas, J. P. Bocquet, R. Brissot, H. R. Faust, Nucl. Phys. A 502 (1989) 233c.
20. S. Steinhäuser, J. Benlliure, C. Böckstiegel, H.-G. Clerc, A. Heinz, A. Grewe, M. de Jong, A. R. Junghans, J. Müller, M. Pfützner, K.-H. Schmidt, Nucl. Phys. A 634 (1998) 89.
21. H. Nifenecker, G. Mariolopoulos, J. P. Bocquet, R. Brissot, Mme Ch. Hamelin, J. Crancon, Ch. Ristori, Z. Phys A 308 (1982) 39.
22. G. Mantzouranis, J. R. Nix, Phys. Rev. C 25 (1982) 918.
23. F. Rejmund, A. V. Ignatyuk, A. R. Junghans, K.-H. Schmidt, Nucl. Phys. A 678 (2000) 215.
24. U. Quade, K. Rudolph, S. Skorka, P. Armbruster, H.-G. Clerc, W. Lang, M. Mutterer, C. Schmitt, J. P. Theobald, G. Gönnenwein, J. Pannicke, H. Schrader, G. Siegert, D. Engelhardt, Nucl. Phys. A 487 (1988) 1.
25. W. Lang, H.-G. Clerc, H. Wohlfarth, H. Schrader, K.-H. Schmidt, Nucl. Phys. A 345 (1980) 34.
26. C. Schmitt, A. Guessous, J. P. Bocquet, H.-G. Clerc, R. Brissot, D. Engelhardt, H. R. Faust, F. Gönnenwein, M. Mutterer, H. Niefenecker, J. Pannicke, Ch. Ristori, J. P. Theobald, Nucl. Phys. A 430 (1984) 21.